Biomed Microdevices (2008) 10:289–298
DOI 10.1007/s10544-007-9135-6

Electroosmotic flow and particle transport in micro/nano nozzles and diffusers

Lei Chen · A. T. Conlisk

Published online: 22 November 2007

Abstract Micro/nano nozzles and diffusers have been used for ionic transport, drug and gene delivery. In this paper, a mathematical model is developed to simulate the electroosmotic flow (EOF) and particle transport in micro/nano nozzles/diffusers. The electrical potential and the flow field are investigated using the lubrication and the Debye–Huckel approximations specially for nanonozzles (overlapped electric double layers) and microdiffusers (thin EDLs) for which experimental results exist. The results show that a pressure field is induced by the presence of EDLs and the magnitude of this induced pressure is proportional to the ratio of the Debye length to the channel half-height. Embedded particles are often employed to illustrate the flow field and thus measure the local fluid velocity. The direction of particle motion is found to be dependent primarily on the particle charge and the wall charge. The calculated particle velocities compare well with experimental data.

Keywords Microfluidics · Nozzle/diffuser · Lubrication theory · Electromigration · Flow field · Particle transport · Ionic transport · Biomolecular transport

L. Chen · A. T. Conlisk (✉)
Department of Mechanical Engineering,
The Ohio State University, 201 W. 19th Avenue,
Columbus, OH 43210, USA
e-mail: Conlisk.1@osu.edu

L. Chen
e-mail: Chen.990@osu.edu

1 Introduction

Electroosmotic flow in micro/nano nozzles and diffusers is important in many applications such as in electrical measurements on living cells (Lehnert et al. 2002) and for the injection and the manipulation of DNA fragments in a mass spectrometer (Luginbuhl et al. 2000). Micro-nozzles have been fabricated using track-etching methods (Lehnert et al. 2002; Luginbuhl et al. 2000; Schultz et al. 2000). Polymer nanotip and nanonozzle arrays have been fabricated using the sacrificial template imprinting (STI) process and uniform polymeric nano-nozzles are produced with sharp end diameters as small as 80 nm (Wang et al. 2005). By growing silica on the internal surface of the nozzle/diffusers, the size of the nozzle can be further reduced to about 10 nm (Wang et al. 2005; Zeng et al. 2005). Since the dimension of a nanonozzle may be comparable to the size of biological macromolecules such as proteins and DNA, it has potential application in single molecule transport, detection, analysis and separation of biomolecules. From the point of view of the present modeling work it is important to note that velocity and concentration profiles are difficult if not impossible to measure in channels less than about 1 micron in their smallest dimension.

A typical geometry is depicted on Fig. 1 (Wang and Hu, private communication). The polymethyl methacrylate (PMMA) nozzle is fabricated by photolithography, followed by replica molding and wet etching respectively. Negatively charged and fluorescence-labeled polystyrene (PS) beads of size from 3 to 40 nm were used to examine the transport of particles in micro-nozzles. The length of the nozzle is 650 μm and the left end and right end heights are

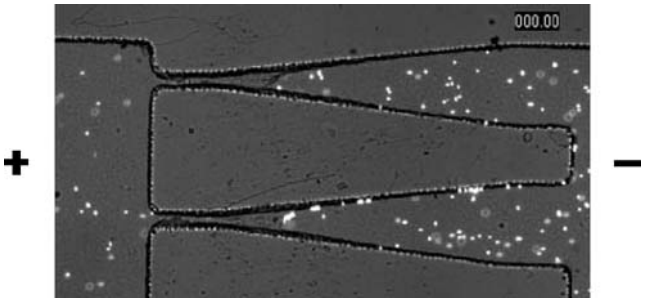

Fig. 1 The geometry of the micro-diffuser in the experiments. The particle donor reservoir is *on the right* and the particle receiver reservoir is *on the left* of the diffuser. The walls are negatively charged and the positive electrode is placed in the particle receiver (*left*). The flow is from left to right and thus it is a diffuser. The polystyrene beads are shown and their motion is from right to left in a direction opposite to the bulk flow

20 and 130 μm, respectively; the nozzle is 40 μm deep and the walls are negatively charged. The particles are immersed in a 0.1 M NaCl solution and an 80 V/cm DC electric field was applied across the tapered channel with the positively charged electrode placed in the particle receiver region (left). Since the walls are negatively charged, cations will always be more populous than anions and will move to the negative electrode, dragging the bulk fluid flow from left to right. Thus in terms of the bulk velocity the device is a diffuser. The negatively charged polystyrene beads move from right to left in a direction opposite to the bulk flow due to electromigration, so for these particles the device is a nozzle. The purpose of this paper is to develop an accurate model to simulate the electroosmotic flow (EOF) and particle transport in these micro/nano nozzles/diffusers. To be consistent, the nozzle and diffuser mentioned in this paper is in terms of the bulk flow.

Much theoretical work has been reported on the study of the electroosmotic flow for parallel plate micro/nano channels with constant wall potential. Early work on the electroosmotic flow was done by Burgeen and Nakache (1964). They determined the velocity and potential for two equally charged ions of valence z in a channel for overlapped electric double layers (EDL). Levine et al. (1975) examined the same problem for both thin and overlapping EDLs. Conlisk et al. (2002) solved the problem for arbitrary ionic mole fractions and have considered the case where there is a potential difference in the direction normal to the channel walls corresponding in some cases to oppositely charged walls. The Debye–Huckel approximation has also been investigated by Conlisk (2005).

Electroosmotic flow in variable geometry channels has been investigated recently. Ghosal (2002) has investigated the electroosmotic flow in slowly varying and periodic cross-sectional geometry and surface potential. He developed asymptotic analytical solutions based on lubrication theory and used a slip boundary condition to approximate the effect of thin double layers. Cervera et al. (2005) have developed a model for electroosmotic flow in conical nanopores. Their model focuses on the ionic transport and the flow field is not considered. Park et al. (2006) have investigated electroosmotic flow through a suddenly constricted cylinder. Due to the induced pressure gradient, eddies are found both in the center of the channel and along the perimeter. The transport of particles in a converging/diverging nanopore has also been investigated by Ghosal (2006). A hydrodynamic model is set up to determine the translocation time of an electrically driven long-chain polymer through a converging nanopore, although the pore was assumed to be uncharged.

All these previous studies use the Helmholtz-Smoluchowski (HS) slip approximation based on the assumption of infinitely thin EDLs. This leads to an EOF with uniform transverse profile in these works. However in view of application to nanoscale nozzle/diffusers, we allow EDLs with finite thickness in our model, which leads to an EOF with a nonuniform transverse profile. It also resolves induced pressure gradients in the problem that can not be resolved by analyses based on the HS approximation.

In this paper, a mathematical model is developed to simulate EOF in these micro/nano nozzle and diffusers; particle transport in nozzle/diffusers is investigated as well as the various regimes of particle and bulk motion based on dimensional analysis. It will be shown that the motion of the particles and the solvent is determined by the magnitude of a single dimensionless parameter, the ratio of the characteristic speeds of electromigration and convection. While spherical polystyrene beads in the experiment are considered here, these results will eventually have application to the motion of DNA.

The plan of the present paper is as follows. In the next section the governing equations of the EOF is discussed and the solution based on the lubrication and Debye–Huckel approximation is derived. Results of EOF in a nano-nozzle and a micro-diffuser are shown next. Particle transport is discussed in the following section and calculated results are compared with the experimental data.

2 Governing equations

Consider a slowly varying channel whose height is nano-constrained as shown in Fig. 2(a) and (b), the

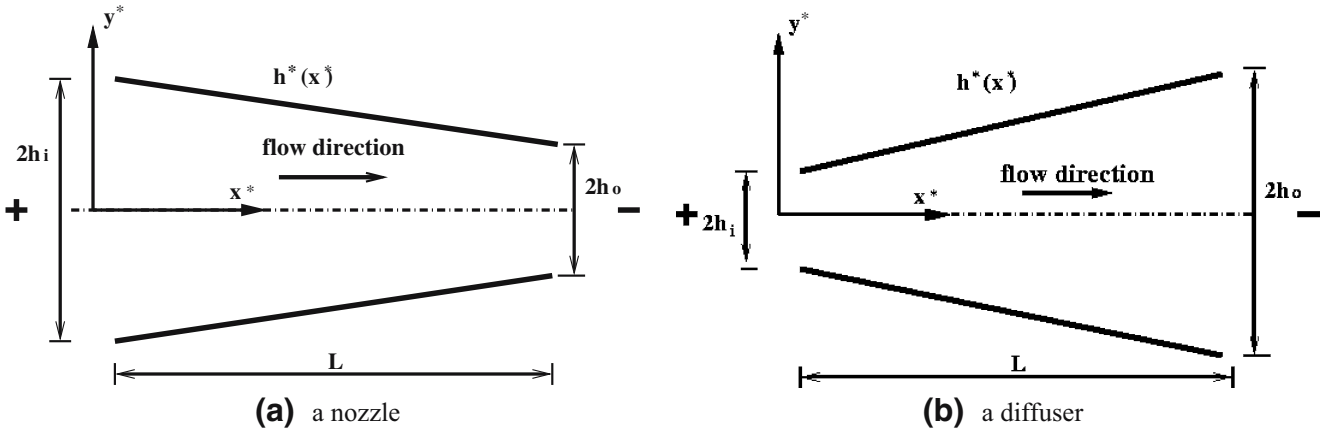

Fig. 2 The geometry of the nozzle/diffuser used for modeling. The walls are negatively charged and for the polarity shown here, the bulk flow is from left to right in both the nozzle and diffuser. (**a**) A nozzle, (**b**) a diffuser

primary direction of fluid flow is in the x-direction. Since there is no significant flow motion in the spanwise direction, for simplicity, the spanwise width of the channel is assumed to be much larger than the height of the channel so the problem can be considered two-dimensional. The length of the channel is L and for the purposes of this paper the channel height is assumed to be linear with

$$h^*(x) = h_i + \frac{h_o - h_i}{L} x^*$$

where h_i, h_o are the half heights of inlet and outlet of the channel and in dimensionless form

$$h(x) = 1 + \frac{h_o - h_i}{h_i} x$$

where $h = \frac{h^*}{h_i}$ and $x = \frac{x^*}{L}$. The walls of the channel are defined by $y = \pm h(x)$.

Electrodes are placed at the inlet and the outlet of the channel and so there is an imposed electric field in the x-direction. The imposed electric field E^* satisfies Maxwell's equations in the form $\nabla \cdot \vec{E}^* = 0$ so that $E_i^*(x)A^*(x) = E_i^*(0)A^*(0)$, where A^* is the dimensional cross-section area of the channel. If the imposed electric field at the inlet $E_i^*(0)$ is taken as the scale of the imposed electric field, the dimensionless imposed electric field is thus $E_i = \frac{1}{h(x)}$. Usually in experiments potential drop is given and the value of this imposed electric field scale $E_i^*(0)$ can be found from the axial integration of $E_i^*(x)$

$$\Delta\phi_i^* = \phi_i^*(L) - \phi_i^*(0) = -\int_0^L E_i^*(x)dx$$

$$= -E_i^*(0)\int_0^L \frac{A^*(0)}{A^*(x)}dx$$

The dimensionless imposed electric field is shown in Fig. 3 for a nozzle (Fig. 2(a)) and a diffuser (experimental setup, as shown in Fig. 2(b)). The potential drop over the length of the nozzle/diffuser corresponds to the value used in the experiments shown in Fig. 1, which is 80 V/cm. It is seen that the magnitude of the electric field is increasing in a nozzle and decreasing in a diffuser in x-direction.

The electric potential due to the presence of EDLs at any point satisfies Poisson's equation

$$\nabla \bullet (\nabla\phi) = -\frac{\rho_e}{\epsilon_e} \tag{1}$$

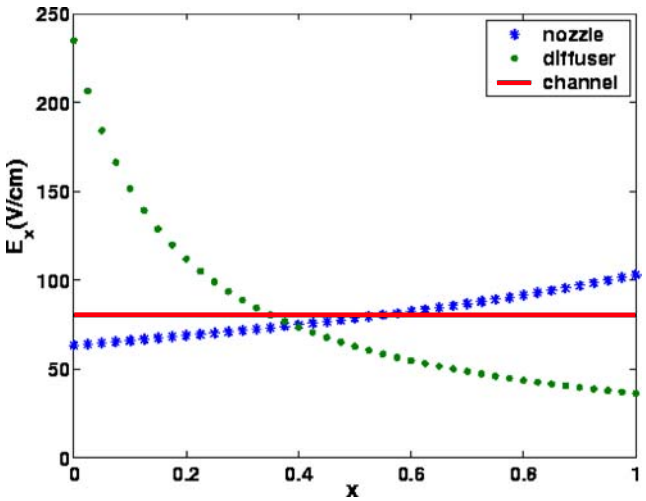

Fig. 3 The dimensionless imposed electric field ($E_{i,x}$) for a nozzle (Fig. 2 (a)) and a diffuser (Fig. 2 (b)). The length of the nozzle is 65 nm; the height at the inlet is 13 nm and the height at outlet is 8 nm. The length of the diffuser is 650 μm; the height at the inlet is 20 μm and the height at the outlet is 130 μm. The potential drop over the length of the nozzle/diffuser corresponds to 80 V/cm. The *solid line* shows the electric field for a straight channel (80 V/cm)

where ρ_e is the volume charge density and ϵ_e is the permittivity of the solution. The charge density is defined by

$$\rho_e = F\sum_i z_i c_i = F c_{\text{total}} \sum_i z_i X_i \tag{2}$$

where c_i, z_i and X_i are the molar concentration, the valence and the mole fraction of species i and F is Faraday's constant. The total concentration c_{total} is defined by

$$c_{\text{total}} = \sum_i c_i + c_{\text{water}}$$

where c_{water} is the molar concentration of water. The non-dimensional equation for the potential due to the EDLs is

$$\frac{\partial^2\phi}{\partial y^2} + \epsilon_1^2\frac{\partial^2\phi}{\partial x^2} = -\frac{\beta}{\epsilon^2}\sum_i z_i X_i \tag{3}$$

where $\beta = \frac{c_{\text{total}}}{I}$ is the ratio of total concentration c_{total} and the ionic strength $I = \sum_i z_i^2 c_i^0$; c_i^0 are known reference concentrations and in this paper they are the concentrations in the upstream reservoir; $\epsilon = \frac{\lambda}{h_i}$ where $\lambda = \sqrt{\frac{\epsilon_e RT}{IF^2}}$ is the Debye length, R is the gas constant and T is the temperature which is taken to be 300 K in the calculation. The potential scale is taken to be $\phi_0 = \frac{RT}{F} = 26$ mV and $\epsilon_1 = \frac{h_i}{L}$. Since $\epsilon_1^2 \ll 1$, Eq. 3 becomes approximately

$$\frac{\partial^2\phi}{\partial y^2} = -\frac{\beta}{\epsilon^2}\sum_i z_i X_i \tag{4}$$

Charged species will respond to three sets of effects: the electrical force from the imposed electric field, diffusion, and the bulk movement of charge carried along by the flow. Therefore the molar flux of species i for a dilute mixture is a vector and is given by

$$\vec{n}_i = -cD_i\nabla X_i + \upsilon_i z_i c F X_i \vec{E}^* + cX_i\vec{u}^* \tag{5}$$

here D_i is the diffusion coefficient; X_i is the mole fraction of species i, which can be either the anion or the cation; υ_i is the mobility, z_i is the valence of species i, $\vec{E}^*$ is the electric field and $\vec{u}^*$ is the velocity of the fluid. The electroosmotic mobility υ_i is defined by the Nernst–Planck equation as

$$\upsilon_i = \frac{D_i}{RT}$$

The mass transfer equation is given by

$$\nabla\cdot\vec{n}_i = 0$$

and the dimensionless governing equation of the species is given by (Conlisk et al. 2002)

$$\frac{\partial^2 X_i}{\partial y^2} + \epsilon_1^2\frac{\partial^2 X_i}{\partial x^2} = Pe\left(\epsilon_1 u\frac{\partial X_i}{\partial x} + v\frac{\partial X_i}{\partial y}\right) + \left(\epsilon_1 z_i\frac{\partial X_i E_x}{\partial x} + z_i\frac{\partial X_i E_y}{\partial y}\right) \tag{6}$$

where, E_x and E_y are the electric fields in the x and y directions and

$$E_x = \frac{h_i E_0 E_{i,x}}{\phi_0} - \epsilon_1\frac{\partial\phi}{\partial x}$$

$$E_y = \frac{h_i E_0 E_{i,y}}{\phi_0} - \frac{\partial\phi}{\partial y}$$

Here Pe is the Peclet number and $Pe = ReSc$, where $Re = \frac{\rho U_0 h_i}{\mu}$ is the Reynolds number and $Sc = \frac{\mu}{\rho D_i}$ is the Schmidt number; E_x^i and E_y^i are the dimensionless components of the imposed electric field in the x and y directions.

The flow field satisfies the continuity equation and Navier–Stokes equations. From conservation of mass, the dimensionless continuity equation is given by

$$\epsilon_1\frac{\partial u}{\partial x} + \frac{\partial v}{\partial y} = 0 \tag{7}$$

The dimensional Navier–Stokes equation is given by

$$\rho\left(\frac{\partial\vec{u}^*}{\partial t^*} + (\vec{u}^*\bullet\nabla)\vec{u}^*\right) = -\nabla p^* + \mu\nabla^2\vec{u}^* + \rho_e\vec{E}^* \tag{8}$$

where ρ is the density of the electrolyte and μ is the fluid viscosity; the pressure field is p^* and the dimensional time is t^*. The convection term on the left hand side of the equation is of the order of Reynolds number and is neglected due to the small $Re \ll 1$. For small aspect ratio $\epsilon_1^2 \ll 1$, the steady state dimensionless streamwise velocity equation is given by

$$\frac{\partial^2 u}{\partial y^2} = \frac{\partial p}{\partial x} - \frac{\beta}{\epsilon^2}\left(\sum_i z_i X_i\right)\left(\frac{1}{h} - \frac{\epsilon_1}{\Lambda}\frac{\partial\phi}{\partial x}\right) \tag{9}$$

where the velocity scale is $U_0 = \frac{\epsilon_e RT E_0}{\mu F}$, the pressure scale is taken to be $p_0 = \frac{\mu U_0}{L}$; and $\Lambda = \frac{E_0 h_i}{\phi_0}$.

The boundary condition for the potential equation is

$$\phi = \phi_w,\ y = \pm h(x)$$

where ϕ_w is the dimensionless wall ζ-potential. The boundary condition for the species equation is that the walls are impermeable to the species and

$$\vec{n}_i\cdot\hat{n}_w = 0,\ y = \pm h(x)$$

$$\vec{n}_i = \left(\frac{\partial X_i}{\partial x} + z_i X_i E_x + Pe X_i u\right)\vec{i} + \left(\frac{\partial X_i}{\partial y} + z_i X_i E_y + Pe X_i v\right)\vec{j}$$

is the flux of the species i and $\hat{n}_w$ is the unit vector normal to the wall. The boundary condition for the velocity field is the no slip boundary condition

$$u = 0,\ v = 0,\ y = \pm h(x)$$

Next solutions for the velocity and potential are obtained in the Debye-Huckel limit.

3 Solutions in the Debye–Huckel limit

The potential, mole fraction and velocity equations are highly nonlinear and coupled, so a full numerical solution needs to be used to find the exact solutions. However, theoretical solutions can be derived based on the Debye–Huckel approximation and lubrication theory. For small potential ($\phi \ll 26$ mV), the potential Eq. 4 becomes (Conlisk 2005)

$$\frac{\partial^2 \phi}{\partial y^2} = \frac{1}{\epsilon^2}\phi \tag{10}$$

and the solution for the potential is

$$\phi = \phi_w \frac{\cosh\frac{y}{\epsilon}}{\cosh\frac{h}{\epsilon}} \tag{11}$$

The velocity can be decomposed into two components: the flow due to the electrical body force u_{eof} and the flow due to the pressure gradient u_{p}. The governing equation for the electroosmotic component of the velocity becomes

$$\frac{\partial^2 u_{\text{eof}}}{\partial y^2} = -\frac{\beta}{\epsilon^2}\left(\sum_i z_i X_i\right)\left(\frac{1}{h} - \frac{\epsilon_1}{\Lambda}\frac{\partial \phi}{\partial x}\right) \tag{12}$$

here $\frac{1}{h}$ is the imposed electric field and $\frac{\epsilon_1}{\Lambda}\frac{\partial \phi}{\partial x}$ is the electric field due to the EDLs. Since the potential gradient in x direction $\frac{\partial \phi}{\partial x}$ is small, this term is neglected. This equation becomes

$$\frac{\partial^2 u_{\text{eof}}}{\partial y^2} = \frac{1}{h}\frac{\partial^2 \phi}{\partial y^2} \tag{13}$$

and the solution of u_{eof} is given by

$$u_{\text{eof}} = \frac{\phi}{h} = \frac{\phi_w}{h}\left(\frac{\cosh\frac{y}{\epsilon}}{\cosh\frac{h}{\epsilon}} - 1\right) \tag{14}$$

Based on the lubrication approximation, the axial pressure gradient is nearly independent of y and the pressure-driven component is given by

$$u_{\text{p}} = \frac{1}{2}\frac{\partial p}{\partial x}\left(y^2 - h^2\right) \tag{15}$$

The total streamwise velocity is then

$$u = u_{\text{eof}} + u_{\text{p}}$$

The v velocity is obtained from the continuity equation as

$$v = -\int_{-h(x)}^{y} \epsilon_1 \frac{\partial u}{\partial x}\mathrm{d}y$$

Substituting the solution of the streamwise velocity ($u = u_{\text{p}} + u_{\text{eof}}$), the transverse velocity v is given by

$$\begin{aligned} v = &-\frac{\epsilon_1}{2}\frac{\mathrm{d}^2 p}{\mathrm{d}x^2}\left(\frac{y^3}{3} - h^2 y - \frac{2}{3}h^3\right) + \epsilon_1 \frac{\mathrm{d}p}{\mathrm{d}x} h h'(y + h) \\ &+ \frac{\epsilon_1 \phi_w h' \sinh\left(\frac{h}{\epsilon}\right)\sinh\left(\frac{y}{\epsilon}\right)}{h\cosh^2\left(\frac{h}{\epsilon}\right)} + \frac{\epsilon \phi_w h' \epsilon_1 \sinh\left(\frac{y}{\epsilon}\right)}{h^2\cosh\left(\frac{h}{\epsilon}\right)} \\ &- \frac{\epsilon_1 \phi_w y h'}{h^2} + \frac{\phi_w h' \epsilon_1 \tanh^2\left(\frac{h}{\epsilon}\right)}{h} \\ &+ \frac{\phi_w \epsilon_1 \epsilon h' \tanh\left(\frac{h}{\epsilon}\right)}{h^2} - \frac{\phi_w \epsilon_1 h'}{h} \end{aligned} \tag{16}$$

The pressure is unknown and the equation for pressure is given by

$$\begin{aligned} \frac{1}{3}h^3\frac{\mathrm{d}^2 p}{\mathrm{d}x^2} + h' h^2 \frac{\mathrm{d}p}{\mathrm{d}x} = &-\frac{\phi_w h'}{h}\tanh^2\left(\frac{h}{\epsilon}\right) \\ &- \frac{\phi_w h' \epsilon}{h^2}\tanh\left(\frac{h}{\epsilon}\right) + \frac{\phi_w h'}{h} \end{aligned} \tag{17}$$

Integrating twice shows

$$p = \frac{\phi_w \epsilon}{h' h^3} - \int_{h_i}^{h} \frac{6\phi_w \epsilon}{h'^2 h^4\left(e^{\frac{2h}{\epsilon}} + 1\right)}\mathrm{d}h + C_1 x + C_2 \tag{18}$$

where C_1 and C_2 are constants of integration and they can be determined by applying the boundary conditions:

$$p = p_{\text{i}},\ x = 0;\ p = p_{\text{o}},\ x = 1.$$

where p_{i} and p_{o} are the pressure in the reservoirs at the inlet and outlet. At this point further integration of this equation is difficult and the solution for pressure has to be found numerically.

For thin EDLs, the electroosmotic component can be simplified as (Conlisk 2005)

$$u_{\text{eof}} = \frac{\phi_w}{h}\left(e^{-\left(\frac{h-y}{\epsilon}\right)} + e^{-\left(\frac{h+y}{\epsilon}\right)} - 1\right) \tag{19}$$

Superimposing the velocities from Eqs. 15 and 19, the total velocity is given by

$$u = \frac{1}{2}\frac{\mathrm{d}p}{\mathrm{d}x}\left(y^2 - h^2\right) + \frac{\phi_w}{h}\left(e^{-\left(\frac{h-y}{\epsilon}\right)} + e^{-\left(\frac{h+y}{\epsilon}\right)}\right) \tag{20}$$

The v-velocity can be obtained as

$$v = -\frac{\epsilon_1}{2}\frac{\mathrm{d}^2 p}{\mathrm{d}x^2}\left(\frac{y^3}{3} - h^2 y - \frac{2}{3}h^3\right) + \epsilon_1 \frac{\mathrm{d}p}{\mathrm{d}x} hh'(y+h) - \frac{\epsilon_1 \phi_w h'}{h^2}(y+h) + \left(\frac{\epsilon \phi_w h' \epsilon_1}{h^2} + \frac{\phi_w h' \epsilon_1}{h}\right) \times \left(e^{-\frac{h-y}{\epsilon}} - e^{-\frac{h+y}{\epsilon}} - e^{-\frac{2h}{\epsilon}} + 1\right) \tag{21}$$

and the pressure solution becomes

$$p = \frac{p_o h_o^2\left(h^2 - h_i^2\right) + p_i h_i^2\left(h_o^2 - h^2\right)}{h^2\left(h_o^2 - h_i^2\right)} - \epsilon\left[\frac{\phi_w}{h'h^3} - \frac{\phi_w\left(h_i^2 + h_i h_o + h_o^2\right)}{h'h^2 h_i h_o (h_i + h_o)} - \frac{\phi_w}{h' h_i h_o (h_i + h_o)}\right] \tag{22}$$

It is seen that the pressure distribution is induced by the inlet and outlet pressure difference (first term in Eq. 22) as well as the presence of the EDLs (second term in

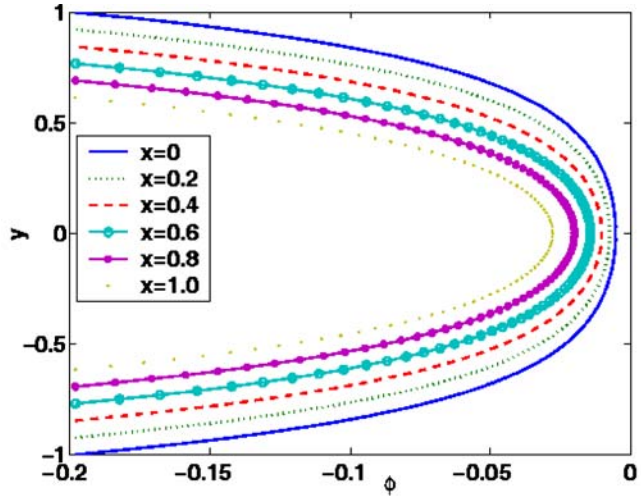

(a) potential

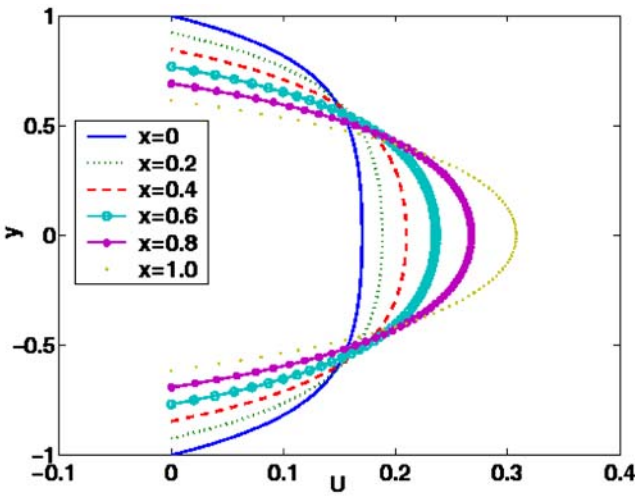

(b) streamwise velocity

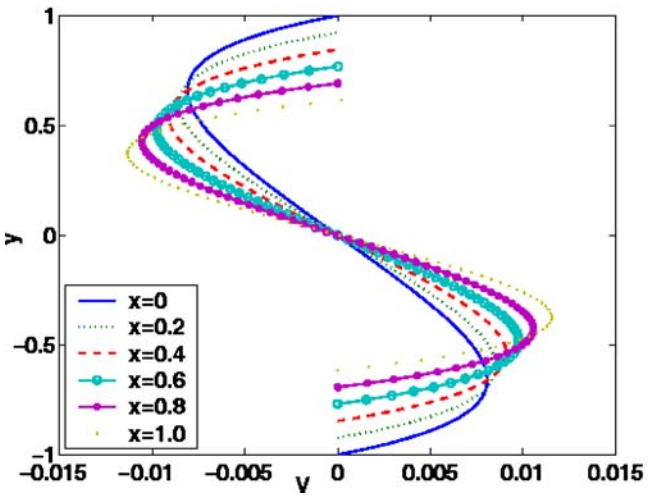

(c) transverse velocity

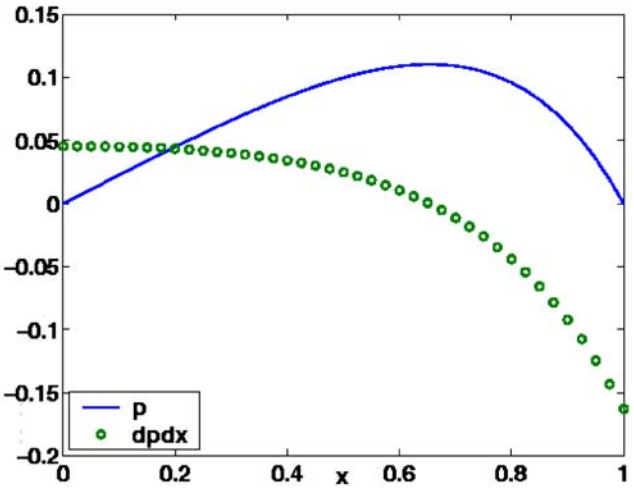

(d) induced pressure and pressure gradient

Fig. 4 Results for electroosmotic flow in the converging nanonozzle. The height of the nozzle is 13 nm at the inlet and 8 nm at the outlet and the length of the nozzle is 65 nm; $\epsilon = 0.19$ and the EDLs are overlapped. The imposed electric field is assumed to be 8,000 V/m and the ζ-potential of the walls is −5 mV. The pressure is zero both at inlet and the outlet and so the pressure shown here is induced by the presence of the EDLs. (**a**) Potential, (**b**) streamwise velocity, (**c**) transverse velocity, (**d**) induced pressure and pressure gradient

Eq. 22). If the inlet and outlet pressure are zero, the pressure in the nozzle/diffuser is proportional to ϵ.

4 Results

Second order finite difference methods are used to discretize the pressure Eq. 17 and the Thomas algorithm is used to solve the system of equations. Figure 4 shows the potential and velocity in the nano-nozzle. The height of the nano-nozzle at the inlet is 13 nm and the length of the nozzle is 65 nm; the height at the outlet is 8 nm and so the parameter $\epsilon_1^2 = 0.04 \ll 1$. The Debye length is 2.5 nm ($\epsilon = 0.19$) and the EDLs are overlapped as shown in the parabolic potential and velocity profiles in Fig. 4. The electrolyte is *NaCl* solution and the concentration in the reservoir is 0.1 M. The imposed electric field is 8,000 V/m. The ζ-potential of the walls is -5 mV which is small enough to apply the solution derived in the previous section based on the Debye–Huckel approximation. The parameters are listed in Table 1.

Since the walls are negatively charged, the fluid flow moves from left to right ($u > 0$) and in terms of the bulk flow, the device is a nano-constrained nozzle. As shown in Fig. 4 the transverse velocity (v) is in the order of ϵ_1 and is small compared to the streamwise velocity (u). The nozzle is assumed to be connected to reservoirs with the pressure zero both at the inlet and the outlet. It is noted that pressure shown here is induced by the presence of the EDLs and the pressure-driven velocity [$u_p \sim O(0.1)$] due to this induced pressure is small compared to the electroosmotic flow velocity [$u_{eof} \sim O(1)$].

Table 1 Values of parameters used for simulations

Parameter	Nano-nozzle	Micro-diffuser
E_0	80 V/cm	80 V/cm
$C^0_{Na^+}$	0.01 M	0.1 M
$C^0_{Cl^-}$	0.01 M	0.1 M
ζ	-5 mV	-15 mV
h_i	13 nm	130 μm
h_o	8 nm	20 μm
L	65 nm	650 μm
ϵ	0.19	5×10^{-5}
Re	2×10^{-6}	0.0035
p_i, p_o	0	0

Note that the concentration of species shown here are reservoir concentrations.

Results for the EOF in the experimental microdiffuser configuration (shown in Fig. 1) having thin EDLs are shown in Fig. 5. The height of the diffuser is 20 μm at the inlet and 130 μm at the outlet and the length of the diffuser is 650 μm; and the parameter $\epsilon^2 = 0.04 \ll 1$. The electrolyte concentration is 0.1 M in the reservoir and the ζ-potential of the PMMA walls is -15 mV (Kirby and Hasselbrink 2004). The Debye length is only 0.7 nm ($\epsilon = 5 \times 10^{-5}$) and the EDLs are very thin compared to the height of the diffuser which can be seen from the plug-like profile of potential and streamwise velocity. The potential rises steeply near the wall; thus to resolve the double layer region, we have further re-scaled our independent variable from $\frac{y}{h}$ to $\frac{y}{(h\epsilon)}$ as shown in the inset of Fig. 5(a). The velocity is a maximum at $x = 0$ and a minimum at $x = 1$ on Fig. 2. The pressure is assumed to be zero both at the inlet and the outlet since the channel is connected to large reservoirs; the pressure shown in Fig. 5(d) is also induced by the presence of EDLs. The magnitude of this induced pressure is small [$O(10^{-5})$] due to the value of small ϵ.

5 Particle transport

A simplified model is used to calculate the velocity of the polystyrene beads shown in Fig. 1. The polystyrene particles are treated as another charged species A immersed in the electrolyte mixture. The flux equation for this species A is

$$\vec{n}^*_A = -D_A \nabla c_A + \upsilon_A z_A F c_A \vec{E}^* + c_A \vec{u}^*$$

and the velocity in the $x-$ direction is

$$u^*_A = -\frac{D_A}{c_A}\frac{\partial c_A}{\partial x} + \upsilon_A z_A F E^*_x + \vec{u}^* \tag{23}$$

Based on the experimental data ($L = 650 \times 10^{-6}$ m and $D_A = 10^{-11}\text{m}^2/\text{s}$ (Pluen et al. 1999); the Stokes-Einstein equation gives similar results for the diffusion coefficient) the magnitude of the first term, the diffusion term is

$$\frac{D_A}{c_A}\frac{\partial c_A}{\partial x} \sim 10^{-11}\frac{\text{m}^2}{\text{s}} / \left(650 \times 10^{-6}\ \text{m}\right)\frac{\Delta c_A}{c_A} \sim 10^{-8}\frac{\Delta c_A}{c_A}\ \frac{\text{m}}{\text{s}}$$

Similarly the second term, the electrical migration term is

$$u_A F z_A E^*_x \sim 4 \times 10^{-15}\frac{\text{mol}}{\text{J}}\ \frac{\text{m}^2}{\text{s}} \times 96{,}500\frac{\text{C}}{\text{mol}}$$
$$\times\ 80\ \text{V}/\left(10^{-2}\ \text{m}\right) z_A \sim 3.9 \times 10^{-5} z_A \frac{\text{m}}{\text{s}}$$

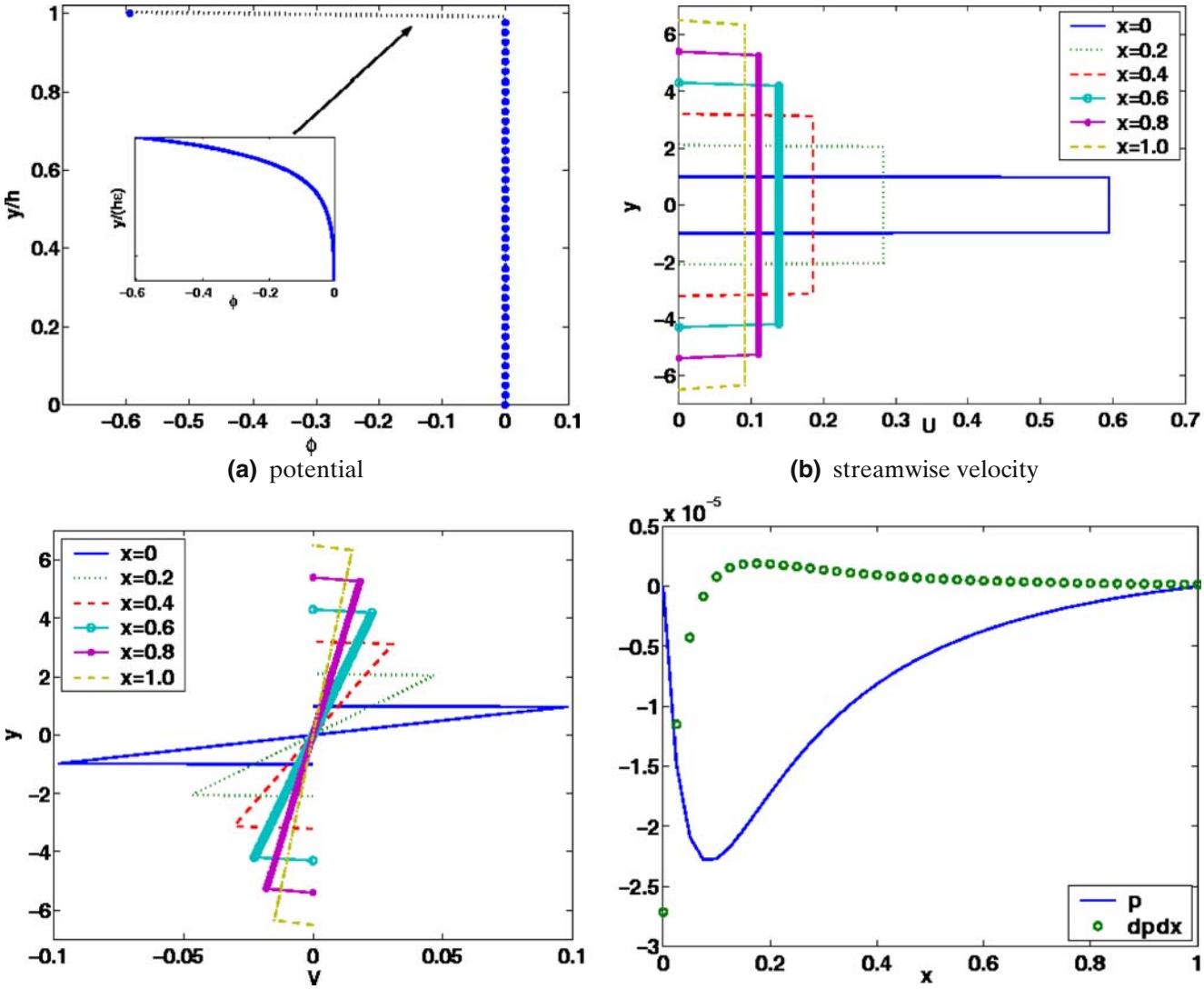

(a) potential

(b) streamwise velocity

(c) transverse velocity

(d) induced pressure and pressure gradient

Fig. 5 Results for electroosmotic flow in the experimental microdiffuser. The height of the diffuser is 20 μm at the inlet and 130 μm at the outlet and the length of the diffuser is 650 μm; $\epsilon = 5 \times 10^{-5}$ and the EDLs are thin compared to the diffuser. The imposed electric field is 8,000 V/m and the ζ-potential is −15 mV. The pressure is zero both at the inlet and the outlet and so the pressure shown here is induced by the presence of the EDLs. In the main frame of (a) the potential profiles have been collapsed to a single curve by using the scaled variable y/h. The inset in the same plot magnifies the EDL region by using the scaled variable $\frac{y}{l}h\epsilon$. (**a**) Potential, (**b**) streamwise velocity, (**c**) transverse velocity, (**d**) induced pressure and pressure gradient

The last term, the convective term is of the order

$$u^* \sim \frac{\epsilon_e E_x^* RT}{F\mu} \sim 1.6 \times 10^{-4} \frac{\text{m}}{\text{s}}$$

Note that the diffusion term is negligible compared to the other two terms while the electrical migration term and the electroosmotic term are comparable. Hence particles can be easily pumped against its concentration gradient. Neglecting the diffusion term, the particle velocity is

$$u_A^* = u_A z_A F E_x^* + \vec{u}^* = u_{\text{EM}} + u_{\text{F}}$$

where u_{EM} is the velocity component due to the electrical migration and u_{F} is the velocity component due to the bulk fluid flow. The particle motion depends on the directions and the magnitudes of these two components.

A reservoir-nozzle system similar to the experimental setup is shown in Fig. 6, which includes a particle donor reservoir and a particle receiver reservoir and a nozzle/diffuser connecting the two reservoirs. Different combinations of wall charge and particle charge determine the direction of fluid flow motion and particle motion.

Consider the transport of an uncharged bio-molecule such as glucose. The velocity within the nozzle responds instantaneously to the inception of the imposed electric field and the glucose, being neutral, is only transported by the bulk fluid motion ($u_{\mathrm{EM}} = 0$). The time scale of this transient period is on the order of millisecond or even smaller. Thus, the total amount of a given species that reaches the receiver is linear with time and this is characteristic of what is termed 'zeroth order release'. If the nozzle wall is positively charged, the fluid flow is from particle donor to the particle receiver and the glucose in solution will be transported into the receiver. If the nozzle is negatively charged, the uncharged species will stay in the particle donor.

Suppose the analyte of interest is a negatively charged species such as albumin or polystyrene beads. The electrostatic force acting on the species will always drive the species to the positive electrode ($u_{\mathrm{EM}} < 0$). The flow direction depends on the nozzle wall charge. If the wall is positively charged, the electromigration term and electroosmotic term will have the same sign ($u_{\mathrm{EM}} < 0, u_{\mathrm{F}} < 0$) and the particles will readily move to the receiver and even adsorb on the walls of the nozzle. Because such a molecule can adsorb to the surface, not all of the particles which originated in the donor will reach the receiver. If the wall is negatively charged, the electromigration term and electroosmotic term have different sign ($u_{\mathrm{EM}} < 0, u_{\mathrm{F}} > 0$) and the particle motion depends on the parameter R_{CE}, which is ratio of the convective term and the electrical migration term:

$$R_{\mathrm{CE}} = \frac{z_A D_A E^*}{\phi_0 U_0}$$

In the experiments shown in Fig. 1, the walls and the particles are both negatively charged ($u_F > 0, u_{\mathrm{EM}} < 0$) and so the particle motion depends on the parameter

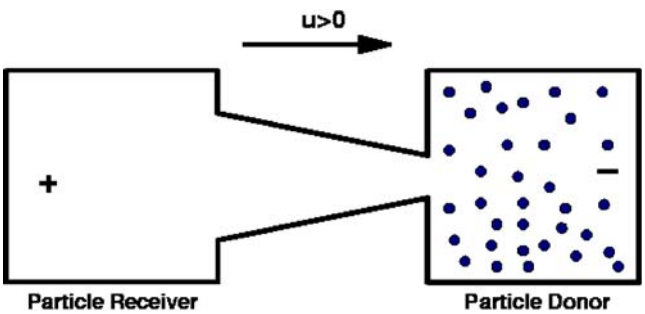

Fig. 6 The reservoir-nozzle system used to analyze particle transport. The *reservoir on the right* is the particle donor reservoir and the *one on the left* is the particle receiver reservoir. Negatively charged particles always tend to move from left to right due to electromigration ($u_{\mathrm{EM}} < 0$)

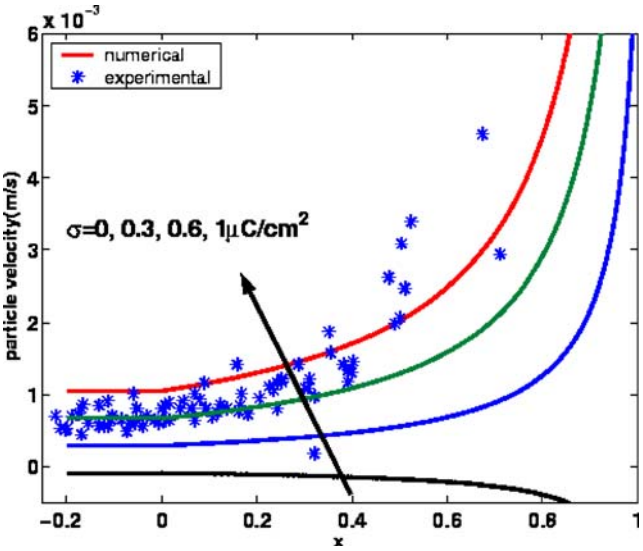

Fig. 7 Comparison of the analytical results and the experimental data (Wang and Hu, private communication). The length of the micro-diffuser is 650 μm; the inlet height is 20 μm and the outlet height is 130 μm. The electric field is 80 V/cm. The ζ-potential of the PMMA walls are −15 mV (Kirby and Hasselbrink 2004). Both the particles and the walls are negatively charged and so $u_{\mathrm{F}} > 0, u_{\mathrm{EM}} < 0$

R_{CE}. For the experimental parameters (Wang and Hu, private communication), $R_{\mathrm{CE}} = 0.02 z_A$. The calculated particle velocity at the nozzle centerline ($y = 0$) is compared with the experimental data in Fig. 7. The experimental data are obtained from visualizing the motion of 80 nm polystyrene beads on the centerline of the nozzle. The dots correspond to the distribution of velocities of the nozzle measured in the experiments and the solid lines are the model velocity for different particle charge. The effective surface charge density can be calculated from $\sigma = \frac{z_A e}{\pi d^2}$ where $e = 1.6 \times 10^{-19} C$ and d is the diameter of the particles. The calculated results compare well with the experimental data for $\sigma = -1 \mu C/cm^2$ and the calculated transit time is 1.65 s. It is also seen that the particles are accelerated near the outlet region due to the higher electric field, which indicates a potential application for drug and gene delivery.

6 Summary

In this paper a model has been established for the electroosmotic flow in a micro/nano nozzle or diffuser. Analytical solutions have been derived based on the lubrication theory and the Debye–Huckel approximation. Particle motion in microdiffusers is investigated and it is found to be dependent on the wall charge,

the particle charge and the parameter R_{CE}. The results shown in this paper can be used to estimate the mass transport of charged/uncharged species in micro/nano nozzles/diffusers which has a potential application for drug and gene delivery. In the future we will extend our study to the transport of DNA in nanonozzles.

References

T. Lehnert, M. Gijs, R. Netzer, U. Bischoff, Appl. Phys. Lett. **81**, 5063 (2002)

P. Luginbuhl, P.-F. Indermuhle, M.-A. Gretillat, F. Willemin, N. de Rooij, D. Gerber, G. Gervasio, J.-L. Vuilleumier, D. Twerenbold, M. Duggelin, et al., Sens. Actuators B **63**, 167 (2000)

G. Schultz, T. Corso, S. Prosser, S. Zhang, Anal. Chem. **72**, 4058 (2000)

S. Wang, C. Zeng, S. Lai, Y.-J. Juang, Y. Yang, L. Lee, Adv. Mater. **17**, 1182 (2005)

C. Zeng, S. Wang, L. J. Lee, Mater. Lett. **59**, 3095 (2005)

Burgeen, Nakache, J. Phys. Chem. **68**, 1084 (1964)

M. Levine, J.R., R. Kenneth, Faraday Trans. II **71**, 1 (1975)

A. T. Conlisk, J. McFerran, Z. Zheng, D. Hansford, Anal. Chem. **74**, 2139 (2002)

A. T. Conlisk, Electrophor. **26**, 1896 (2005)

S. Ghosal, J. Fluid Mech. **459**, 103 (2002)

J. Cervera, B. Schiedt, P. Ramirez, Europhys. Lett. **71**, 35 (2005)

S. Y. Park, C. J. Russo, D. Branton, H. A. Stone, J. Colloid Interface Sci. **197**, 832 (2006)

S. Ghosal, Phys. Rev. E **74**, 041901 (2006)

B. J. Kirby, E. F. Hasselbrink, Electrophor. **25**, 203 (2004)

A. Pluen, P. A. Netti, R. K. Jain, D. A. Berk, Biophys. J. **77**, 542 (1999)